Robotica (2000) volume 18, pp. 347–360. Printed in the United Kingdom © 2000 Cambridge University Press

Kinematic modelling and trajectory planning for a tele-laparoscopic manipulating system

Ali Faraz and Shahram Payandeh

Experimental Robotics Laboratory (ERL), School of Engineering Science, Simon Fraser University, Burnaby, British Columbia V5A 1S6 (Canada)
E-mail: shahram@cs.sfu.ca

(Received in Final Form: September 4, 1999)

SUMMARY
This paper addresses the kinematic modelling, solutions and trajectory planning of a tele-laparoscopic manipulator. This type of manipulator can be used in remote positioning of laparoscopic tools through tele-operating system. Specifically the paper models kinematics of a typical manipulating system which can be used in such tele-surgery. Inverse kinematics solutions are also obtained for two kinematically constraint motions which are part of a typical trajectory of the laparoscopic tools. These are fixed axis rotation of the tool and its straight line motion. Simulation results are presented to demonstrate the validity of such models and solutions.

KEYWORDS: Tele-laparoscopic system; Kinematic modelling; Trajectory planning

1. INTRODUCTION

The remote manipulation in laparoscopy introduces kinematic motion problems described as: (a) spherical movements of tool at the port of entry on the abdomen, and (b) lack of dexterity inside the abdomen. There are a number of works in the literature addressing robotic applications for laparoscopy, which can be categorized in two main types:

Automated Positioners. This type is basically a positioner for laparoscopic tools and a navigating system which in addition to locking tools in a desired configuration, it also can reposition the tool to a previously defined location (e.g. for changing the angle of endoscopic view to a previously stored orientation). This type of positioner is also commercially available by Computer Motion Inc. (AESOP units).[1–3] Taylor *et al*,[4] have developed an automated positioner with a parallelogram configuration to provide remote center of rotation for laparoscopic tools. Also the commercial development (EndoSista) by Armstrong Projects, is a specially designed positioner to control laparoscopic view directly by head movements of the surgeon.

Tele-Operated Extenders. One of the main areas of potential application for robotic extenders in laparoscopy, is in the field of tele-operated master-slave system. This is due to the fact that laparoscopic surgery with inverse hand motion and limited force sensing is very unnatural to control and physically demanding for the surgeons. As a result, this motivates to develop tele-operated extenders so that the surgeon can control the direct motion of the tool's tip on the monitor, instead of reverse motion at the handle which is the case in manual operations currently performed.[5] There are also other research works proposing the general concept of tele-surgical workstations for laparoscopy, which are based on master-slave tele-operated systems.[6,7] However, there has not been any specific design for implementation or experimental developments for laparoscopy. The only tele-operated surgical development belongs to SRI International.[8] However their current design configuration is only suitable for open surgery, since it does not have any DOF to perform spherical movements at the port of entry which is a primary requirement for laparoscopy.

This paper presents a kinematic model and solution to a laparoscopic manipulating system which can be used in the context of automated positioning systems and/or tele-operating system. The paper is organized as follows: Section (2) presents the mechanical configuration of the system; Section (3) presents the kinematic model of the manipulating system and the inverse kinematic solutions; Section (4) presents solutions for trajectory generation for two types of motions: (a) fix-point rotation and (b) linear motion. Finally Section (5) presents some concluding remarks.

2. CONFIGURATION OF ROBOTIC EXTENDERS

The design configuration of robotic extenders for laparoscopic applications should generally meet the two primary requirements: (a) to comply with the kinematic constraint at the port of entry; (b) to provide sufficient DOF inside the abdomen for the specific surgical task.

Generally laparoscopic positioners are used either for positioning the laparoscope, or surgical tools (such as retractors, graspers, etc), which both cases require two positioning DOF (*i.e.* θ_1, and θ_2, Figure 1). In the case of laparoscope, 2 additional DOF at the port of entry are needed. One DOF for the rotational adjustment of laparoscope around its longitudinal axis (θ_3), so that the image on the monitor obtains the upright orientation. The second DOF for translating the laparoscope in and out of abdomen for zooming purposes. Also, in the case of surgical tools same 2 DOF are required for proper orientation and axial reach at the surgical site. Therefore for this type of positioner, generally a total of 4 DOF (*i.e.* θ_1, θ_2, θ_3, and l at the port of entry, Figure 1) is adequate. The design of

https://doi.org/10.1017/S026357479900209X Published online by Cambridge University Press

extender can be implemented by adding the 2 actuated joints (*i.e.* C, and D) to the distal end of concentric spherical mechanism with actuated joints A and B, as shown schematically in Figure 1.[2,3]

For performing surgical tasks by a tele-operation system similar to the current laparoscopic tools with rigid stem, then the slave robotic extender only requires 4 DOF as described above. However, by incorporating flexible stem tools as an added end-effector to the end of the extender (Figure 2), it is possible to have full rank 6 DOF (i.e. with the two addition DOF for orientation, θ_4 and θ_5) to manipulate the surgical tissues without any kinematic constraint. This would be an complementry step compared to the above design (Figure 1). In Figure 2, joint E provides actuation for the joint on stem (*i.e.* θ_4). A flexible shaft can transmit both of the actuations F and G, for rotation (*i.e.* θ_5), and grasping action, respectively.

In the following section, kinematics of the above design configuration are further studied, which includes homogeneous coordinates transformation, forward and inverse kinematics, as well as singularity study, and constraint motion of such robotic extenders.

3. KINEMATICS OF THE EXTENDER

The kinematic aspects of the above laparoscopic extender with 6 DOF is studied in this section. The coordinates transformations from the base to the distal end of extender based on the coordinates of joints are considered. This is useful in order to be able to determine the tracking of end-point trajectory, or any other intermediate points. For this purpose, initially, we have to define all the links parameters and joints variables. A commonly used convention for selecting frames of reference in robotic applications is Denavit-Hartenberg (or D-H) convention. In this convention, various parameters of link/joint i are: a_i its length, α_i twist angle, d_i offset, and θ_i the joint angle (Figure 2). Based on this convention, the parameters of the laparoscopic extender (Figure 3) a_i, α_i, d_i and θ_i are given in Table I. The homogeneous transformation $\mathbf{A}_i$ along each link is represented by:

$$\mathbf{A}_i = Rot_{z,\theta i} Trans_{z,di} Trans_{x,ai} Rot_{x,\alpha i}$$

$$= \begin{bmatrix} C\theta_i & -S\theta_i C\alpha_i & S\theta_i S\alpha_i & a_i C\theta_i \\ S\theta_i & C\theta_i C\alpha_i & -C\theta_i S\alpha_i & a_i S\theta_i \\ 0 & S\alpha_i & C\alpha_i & d_i \\ 0 & 0 & 0 & 1 \end{bmatrix}$$

For each joint, by substituting the values of parameters from Table I, in the above equation, it provides us with individual transformations as follows:

$$\mathbf{A}_5 = \begin{bmatrix} C_4 & 0 & S_4 & 0 \\ S_4 & 0 & -C_4 & 0 \\ 0 & 1 & 0 & 0 \\ 0 & 0 & 0 & 1 \end{bmatrix} \qquad \mathbf{A}_6 = \begin{bmatrix} C_5 & -S_5 & 0 & 0 \\ S_5 & C_5 & 0 & 0 \\ 0 & 0 & 0 & l_e \\ 0 & 0 & 0 & 1 \end{bmatrix}$$

Therefore, the total transformation from the coordinate frame of grasper $\mathbf{X}_6$ to the base from $\mathbf{X}_0$ at the port of entry would be:

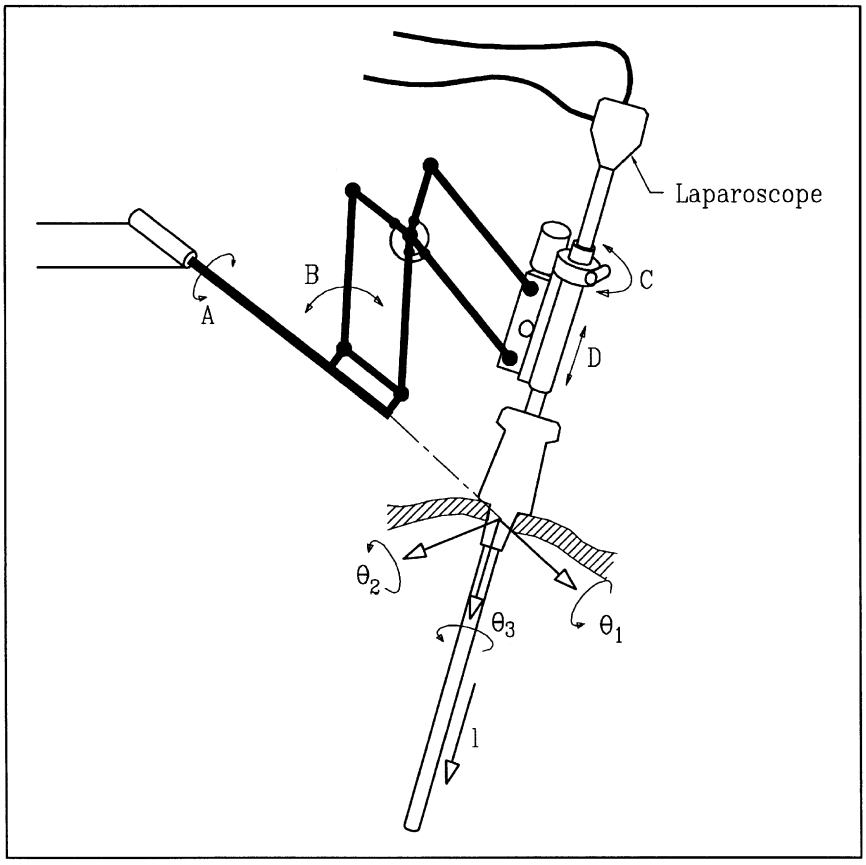

Fig. 1. Schematic of the robotic extender with 4 DOF.

https://doi.org/10.1017/S026357479900209X Published online by Cambridge University Press

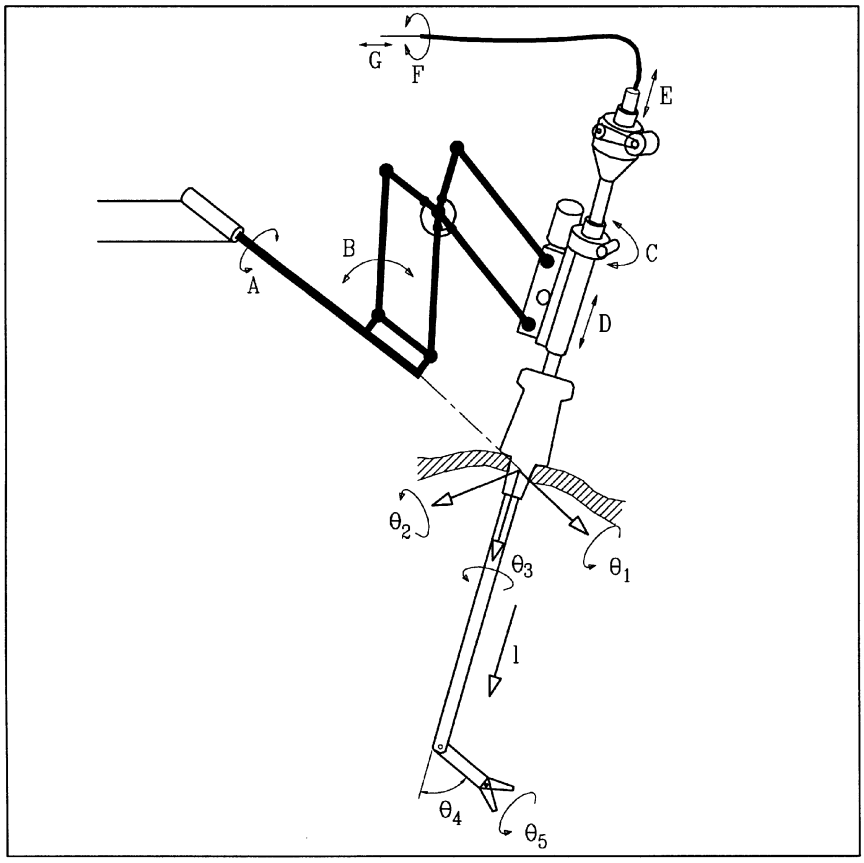

Fig. 2. Schematic of the robotic extender with 6 DOF.

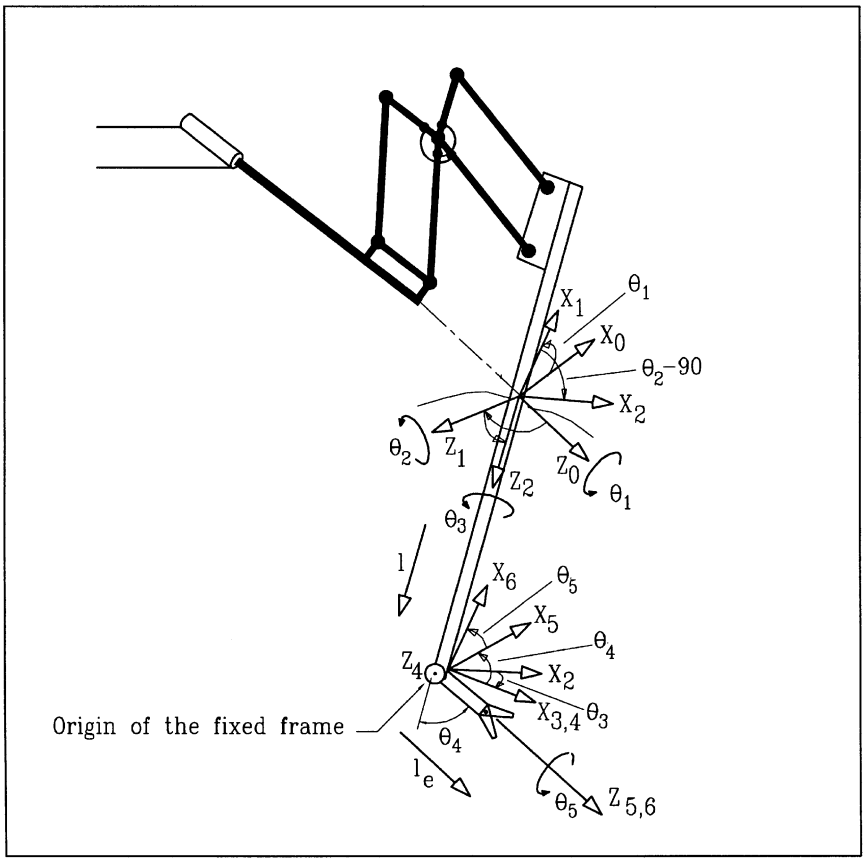

Fig. 3. Joints coordinate frames of the extender and their transformations.

https://doi.org/10.1017/S026357479900209X Published online by Cambridge University Press

Table I. The parameters of laparoscopic extender

Link/Joint	a_i	α_i	d_i	θ_i
1	0	$-90°$	0	θ_1
2	0	90°	0	$\theta_2 - 90°$
3	0	0	0	θ_3
4	0	$-90°$	l	0
5	0	90°	0	θ_4
6	0	0	l_e	θ_5

$$\mathbf{X}_0 = \mathbf{A}_1\mathbf{A}_2\mathbf{A}_3\mathbf{A}_4\mathbf{A}_5\mathbf{A}_6\mathbf{X}_6 = \begin{bmatrix} a_{11} & a_{12} & a_{13} & a_{14} \\ a_{21} & a_{22} & a_{23} & a_{24} \\ a_{31} & a_{32} & a_{33} & a_{34} \\ a_{41} & a_{42} & a_{43} & a_{44} \end{bmatrix} \mathbf{X_6}$$

Where,

$$a_{11} = (C_1S_2C_3 - S_1S_3)C_4C_5 + C_1C_2S_4C_5 - (C_1S_2S_3 + S_1C_3)S_5$$

$$a_{21} = (S_1S_2C_3 + C_1S_3)C_4C_5 + S_1C_2S_4C_5 - (S_1S_2S_3 - C_1C_3)S_5$$

$$a_{31} = C_2C_3C_4C_5 - S_2S_4C_5 - C_2S_3S_5$$

$$a_{41} = 0$$

$$a_{12} = -(C_1S_2C_3 - S_1S_3)C_4S_5 - C_1C_2S_4C_5 - (C_1S_2S_3 + S_1C_3)C_5$$

$$a_{22} = -(S_1S_2C_3 + C_1S_3)C_4S_5 - S_1C_2S_4S_5 - (S_1S_2S_3 - C_1C_3)C_5$$

$$a_{32} = -C_2C_3C_4S_5 + S_2S_4S_5 - C_2S_3C_5$$

$$a_{42} = 0$$

$$a_{13} = (C_1S_2C_3 - S_1S_3)S_4 - C_1C_2C_4$$

$$a_{23} = (S_1S_2C_3 + C_1S_3)S_4 - S_1C_2C_4$$

$$a_{33} = C_2C_3S_4 + S_2C_4$$

$$a_{43} = 0$$

$$a_{14} = (C_1S_2C_3 - S_1S_3)S_4l_e - C_1C_2C_4l_e - C_1C_2l$$

$$a_{24} = (S_1S_2C_3 + C_1S_3)S_4l_e - S_1C_2C_4l_e - S_1C_2l$$

$$a_{34} = C_2C_3S_4l_e + S_2C_4l_e + S_2l$$

$$a_{44} = 1$$

and C_i and S_i are abbreviation of *Cos* θ_i, and *Sin* θ_i respectively.

3.1. Jacobian formulation

The kinematics and control related aspects of any robotic manipulator requires the formulation or mapping of the velocity state of end-effector (e.g. (ω, $\mathbf{v}$) expressed with respect to a frame of reference) to the velocity state of joints ($\dot{\theta}_i$). This relationship can be expressed as:

$$\begin{bmatrix} \omega_x \\ \omega_y \\ \omega_z \\ V_x \\ V_y \\ V_z \end{bmatrix} = \begin{bmatrix} w_1^x & w_2^x & w_3^x & w_4^x & w_5^x & w_6^x \\ w_1^y & w_2^y & w_3^y & w_4^y & w_5^y & w_6^y \\ w_1^z & w_2^z & w_3^z & w_4^z & w_5^z & w_6^z \\ (w_1\times r_1)^x & (w_2\times r_2)^x & (w_3\times r_3)^x & (w_4\times r_4)^x & (w_5\times r_5)^x & (w_6\times r_6)^x \\ (w_1\times r_1)^y & (w_2\times r_2)^y & (w_3\times r_3)^y & (w_4\times r_4)^y & (w_5\times r_5)^y & (w_6\times r_6)^y \\ (w_1\times r_1)^z & (w_2\times r_2)^z & (w_3\times r_3)^z & (w_4\times r_4)^z & (w_5\times r_5)^z & (w_6\times r_6)^z \end{bmatrix} \begin{bmatrix} \dot{\theta}_1 \\ \dot{\theta}_2 \\ \dot{\theta}_3 \\ \dot{l} \\ \dot{\theta}_4 \\ \dot{\theta}_5 \end{bmatrix} \quad (1)$$

Where $w_i = [w_i^x, w_i^y, w_i^z]^T$ is a unit vector in the direction of the axis of joint i, and r_i is the connecting vector of origin of axis i to the reference point of, for example, the end-effector.

By definition the matrix on the right hand side of Eq. (1), which is called *Jacobian* of the manipulator. Finding Jacobians in robots with relatively high DOF results in two main difficulties as follows: (a) normally the Jacobian would be a $6\times N$ matrix (where N is the number of joints or DOF in the manipulator) which creates computational load at each iteration of incremental movement along the path of trajectory even in forward kinematics; (b) for inverse kinematics, inverting the Jacobian numerically requires intensive computation.

In this paper, an approach based on the screw geometry for obtaining the Jacobian of the manipulator is followed.[9] This approach offers a closed-form and compact representation of the Jacobian matrix. In summary, the approach obtains Jacobian with much simpler structures which provides closed form analytical solution for inverse kinematics ($\dot{\theta}_i$).

In this approach, the formulation of Eq. (1) is slightly altered, and instead of the velocity of the reference point of end-effector $\mathbf{v}$ with respect to the base frame $\mathbf{X}_0$, μ the velocity of the (virtual) point in the hand is obtained, with respect to an intermediate frame on the kinematic structure of the manipulator. In general we can write:

$$\mu = \mathbf{v} - \omega \times \mathbf{a} \quad (2)$$

where for example, $\mathbf{a}$ is the position of the end-effectors reference point (Figure 4), relative to the fixed frame $\mathbf{X}_0$.

In the kinematic model of this paper, the fixed frame is transferred to an intermediate joint instead of at the base of manipulator. In this paper, the fixed frame is chosen to be at joint Z_4 (Figure 4). This provides us with the following compact kinematic equation and Jacobian (for detail derivation see Appendix A):

$$\begin{bmatrix} \omega_x \\ \omega_y \\ \omega_z \\ \mu_x \\ \mu_y \\ \mu_z \end{bmatrix} = \begin{bmatrix} C_2C_3 & S_3 & 0 & 0 & 0 & S_4 \\ -S_2 & 0 & -1 & 0 & 0 & -C_4 \\ -C_2S_3 & C_3 & 0 & 0 & 1 & 0 \\ -lC_2S_3 & lC_3 & 0 & 0 & 0 & 0 \\ 0 & 0 & 0 & -1 & 0 & 0 \\ -lC_2C_3 & -lS_3 & 0 & 0 & 0 & 0 \end{bmatrix} \begin{bmatrix} \dot{\theta}_1 \\ \dot{\theta}_2 \\ \dot{\theta}_3 \\ \dot{l} \\ \dot{\theta}_4 \\ \dot{\theta}_5 \end{bmatrix} \quad (3)$$

The above equation of forward kinematics is simulated for the full range of motion of all joints (*i.e.* from coordinates [$-75°$, $-75°$, $-180°$, 80*mm*, $-120°$, $-180°$] to [75°,75°, 180°, 280*mm*, 120°, 180°]) with constant speed. The constant velocity of each joint is selected so that the full range of travel of the joint would be completed within 10 seconds (Figure 5a to 5f, *i.e.* $\dot{\theta}_1 = \dot{\theta}_2 = 15°/s = 0.262 rad/s$, $\dot{\theta}_3 = \dot{\theta}_5 = 36°/s = 0.628 rad/s$, $\dot{\theta}_4 = 24°/s = 0.419 rad/s$, and $\dot{l} = 20 mm/s$). The velocity state of the grasping point at the tip of extender (relative to the fix frame $\mathbf{X}_0$, Figure 3) is calculated based on Eq. 3, and 2, as shown in Figure 5g to 5l.

https://doi.org/10.1017/S026357479900209X Published online by Cambridge University Press

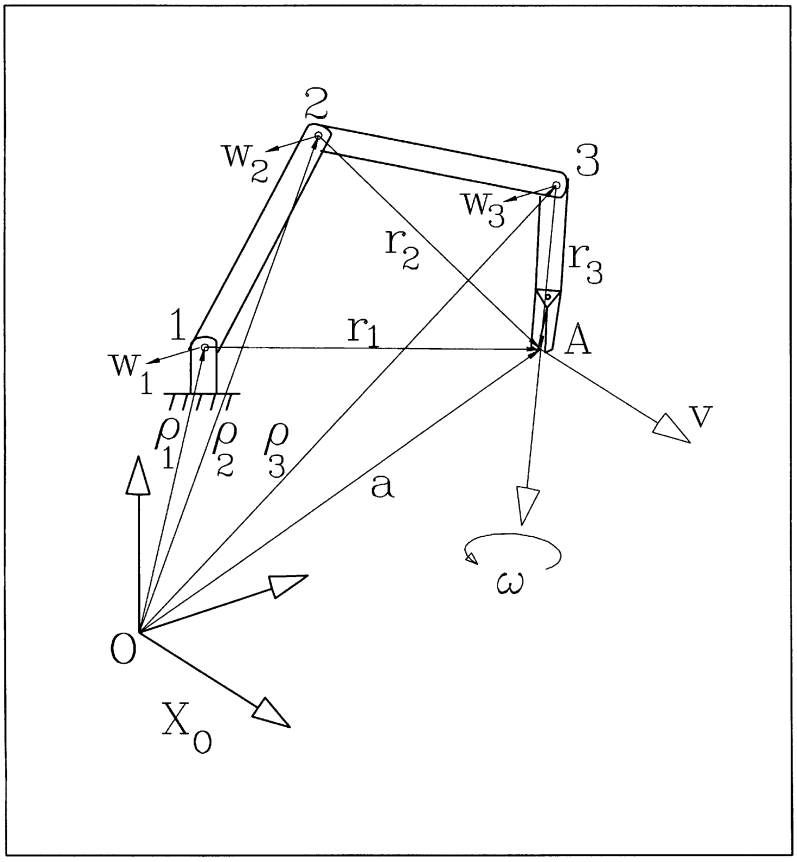

Fig. 4. Geometric parameters *p* and **a** for a 3 DOF manipulator.

Now, by having the Jacobian it is possible to study conditions of the extender. Generally, manipulators Jacobian is a function of its configuration, and singularity occurs when the $det|\mathbf{J}|=0$, which means the inverse of Jacobian does not exist at that configuration. Hence at singularity, for bounded velocities of end-effector it requires unbounded joint(s) velocities, and since this is not possible for any actuator, consequently the manipulator looses at least one of its DOF.

To obtain the determinant, the Jacobian is reduced by its 3rd, 4th, and 5th columns, which yields following further simplifications:

$$|\mathbf{J}| = \begin{vmatrix} C_2C_3 & S_3 & S_4 \\ -lC_2S_3 & lC_3 & 0 \\ -lC_2C_3 & -lS_3 & 0 \end{vmatrix} = l^2C_2S_4 = 0 \qquad (4)$$

Then singularity occurs when: $l=0, \theta_2=\pm 90°$, $\theta_4=0$, and 180°. However based on the surgical conditions in laparoscopy, the normal range for the parameters are[10] $l>80mm$, $-75°<\theta_2<+75°$, and $-120°\leqslant\theta_4\leqslant 120°$. Therefore, the only possibility for the occurrence of singularity is when $\theta_4=0$, that in this case, the shank of the flexible stem is fully straight without any bend, and the axes 3, and 5 are collinear. This means, at the singularity, the manipulator looses 1 DOF in dexterity (of orienting the grasper toward the surgical site). To avoid the singularity, then $\theta_4\neq 0$ must be satisfied, and for dexterous operation of the extender θ_4 should not approach the zero value by remaining in a higher range (e.g. $\theta_4>30°$).

3.2. Inverse kinematics

The compact formulation of forward kinematics (3) makes it possible to be solved analytically, in order to obtain the inverse kinematics as follows:

$$\begin{cases} C_2C_3\dot{\theta}_1+S_3\dot{\theta}_2+S_4\dot{\theta}_5=\omega_x \\ -S_2\dot{\theta}_1-\dot{\theta}_3-C_4\dot{\theta}_5=\omega_y \\ -C_2S_3\dot{\theta}_1+C_3\dot{\theta}_2+\dot{\theta}_4=\omega_z \\ -lC_2S_3\dot{\theta}_1+lC_3\dot{\theta}_2=\mu_x \\ -\dot{l}=\mu_y \\ -lC_2C_3\dot{\theta}_1-lS_3\dot{\theta}_2=\mu_z \end{cases}$$

$$\begin{cases} \dot{\theta}_1=-(S_3\mu_x+C_3\mu_z)/lC_2 \\ \dot{\theta}_2=(C_3\mu_x-S_3\mu_z)/l \\ \dot{\theta}_3=-(C_4/S_4)\omega_x-\omega_y+(S_2S_3/lC_2)\mu_x \\ \qquad -(C_4/lS_4-C_3S_2/lC_2)\mu_z \\ \dot{l}=-\mu_y \\ \dot{\theta}_4=\omega_z-\mu_x/l \\ \dot{\theta}_5=(\omega_x+\mu_z/l)/S_4 \end{cases}$$

https://doi.org/10.1017/S026357479900209X Published online by Cambridge University Press

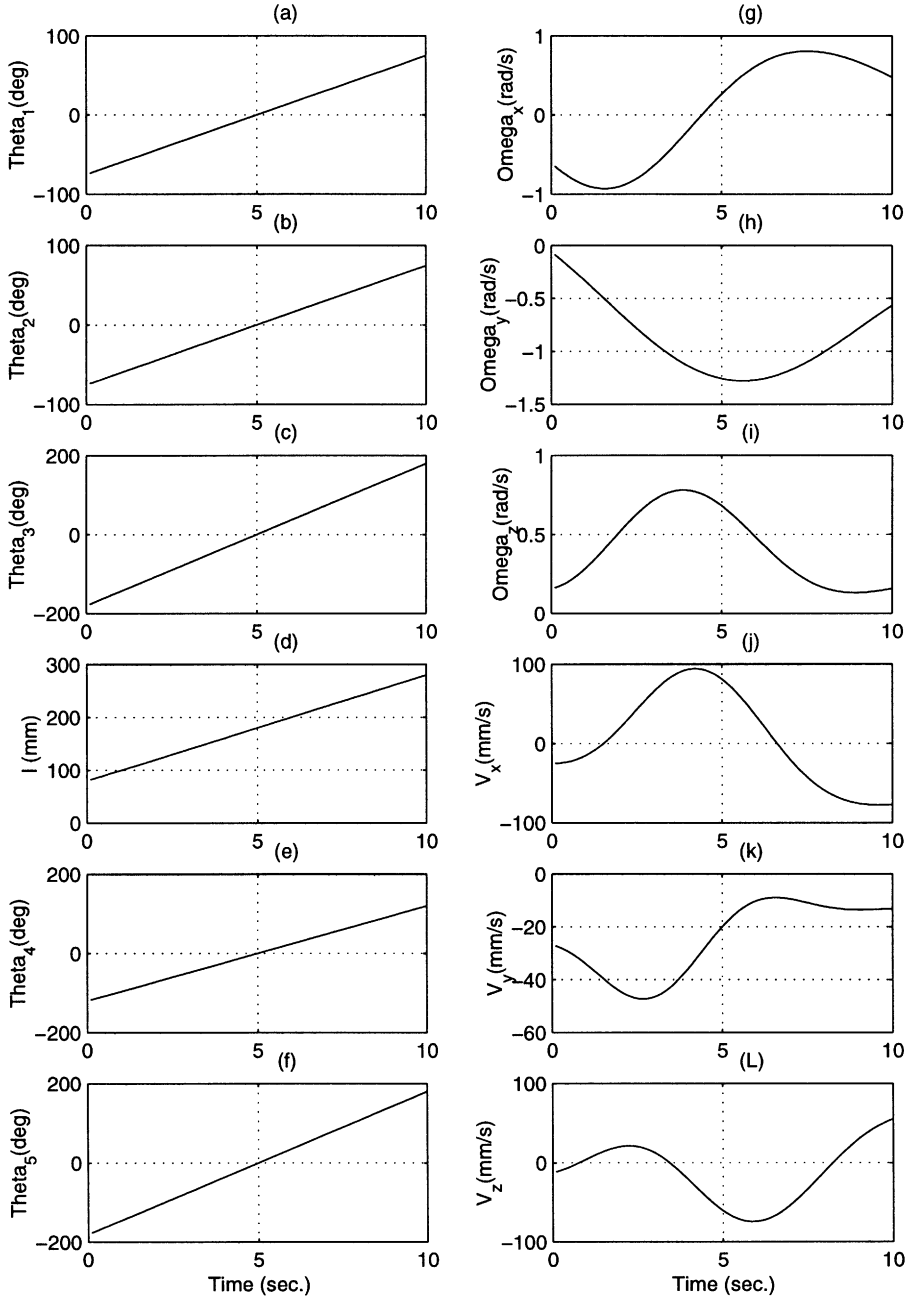

Fig. 5. Forward kinematics simulation.

Which can be written as $\dot{\theta}=\mathbf{J}^{-1}\dot{X}$, or:

$$\begin{bmatrix} \dot{\theta}_1 \\ \dot{\theta}_2 \\ \dot{\theta}_3 \\ \dot{l} \\ \dot{\theta}_4 \\ \dot{\theta}_5 \end{bmatrix} = \begin{bmatrix} 0 & 0 & 0 & -\frac{S_3}{lC_2} & 0 & -\frac{C_3}{lC_2} \\ 0 & 0 & 0 & \frac{C_3}{l} & 0 & -\frac{S_3}{l} \\ \frac{-C_4}{S_4} & -1 & 0 & \frac{S_2S_3}{lC_2} & 0 & -\frac{C_4}{lS_4}-\frac{S_2C_3}{lC_2} \\ 0 & 0 & 0 & 0 & -1 & 0 \\ 0 & 0 & 1 & -\frac{1}{l} & 0 & 0 \\ \frac{1}{S_4} & 0 & 0 & 0 & 0 & \frac{1}{lS_4} \end{bmatrix} \begin{bmatrix} \omega_x \\ \omega_y \\ \omega_z \\ \mu_x \\ \mu_y \\ \mu_z \end{bmatrix} \quad (5)$$

The above equation of inverse kinematics is simulated by using the motion of endpoint (*i.e.* $[\omega, \mu]$) from the previous simulation (*i.e.* Figures 6g to 6l), as the input for Eq 5. The virtue of doing so is to verify if the inverse kinematics can be indeed reproduce the initial constant speeds used as input to the forward kinematics. As shown in Figure 6g to 6l, the output of inverse kinematics (Eq. 5) is identical to the input of forward kinematics (Figures 5a to 5f), with the only difference that, at $\theta_4=0$ (t=5 sec), for bounded input, the output values of $\dot{\theta}_3$, and $\dot{\theta}_5$ are unbounded. This is caused by the singularity at $\theta_4=0$, when the two axes θ_3, and θ_4 are collinear, and the extender looses 1 DOF in angular motion at the end-point.

4. CONSTRAINED MOTION

Robotic manipulators usually have to work with specific geometrical constraints defined through their trajectories.

https://doi.org/10.1017/S026357479900209X Published online by Cambridge University Press

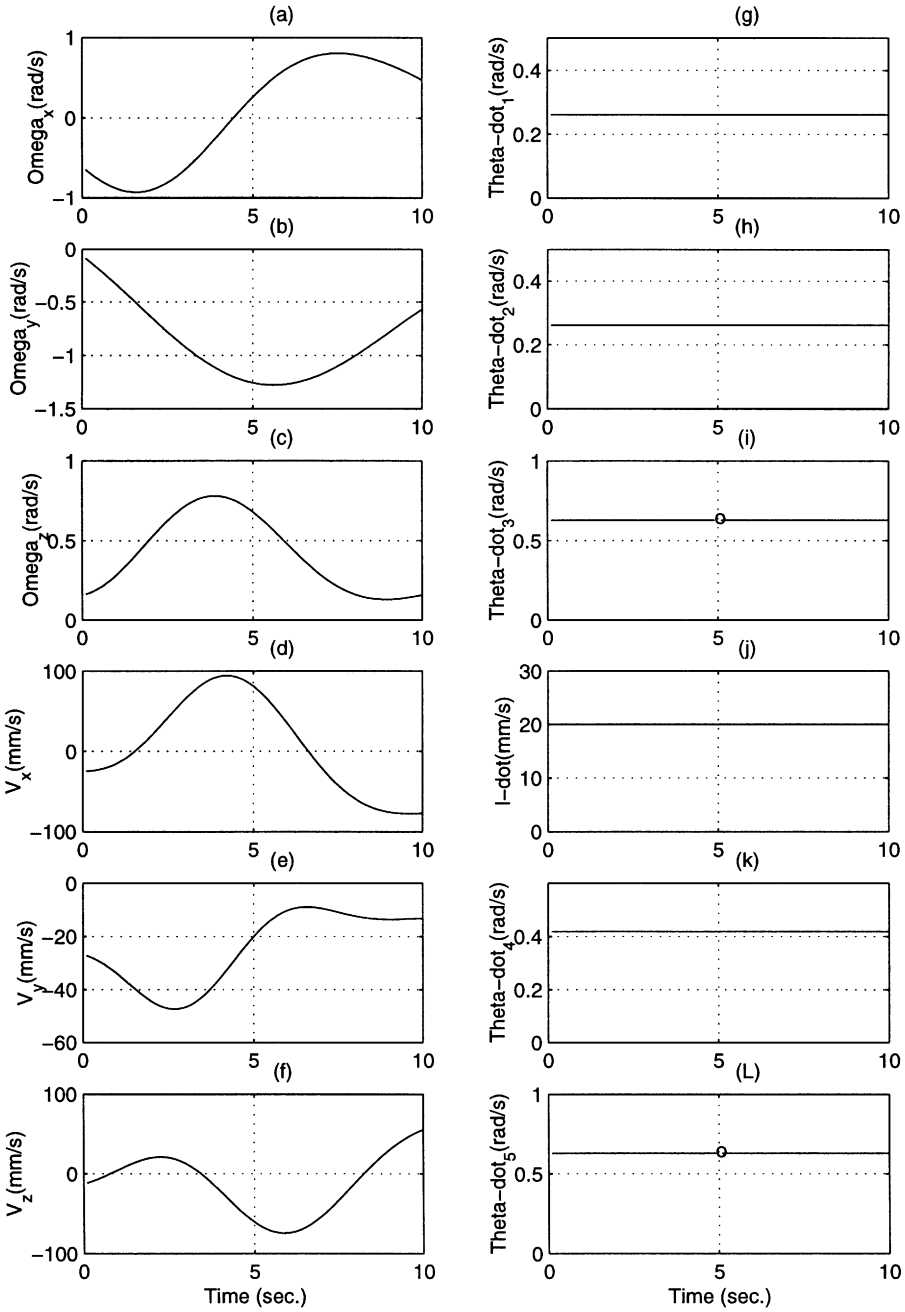

Fig. 6. Inverse kinematics simulation.

For example, to perform the task of painting on a flat surface, the end-effector has to move in an equidistant plane parallel to the painting surface, or in welding not only the end-effector has to follow the exact path of the seam, also it has to remain at a specific orientation with respect to the seam.

In laparoscopy there are constrained motions, such as manipulation of tissue at an incision. In this case, basically the surgeon grasps the tissue with the extender, then changes its orientation while the position of the grasping point should remain the same in order to prevent any undesirable pull or tear of the tissue. This constrained motion requires freedom of movement in orienting the extender, while its tip has a *fixed position* in the work space (Figure 7).

On the other hand, there is another type of constrained motion in laparoscopy related to tasks that require *fixed orientation*, such as suturing. In this task, the needle should penetrate the tissue while its orientation should remain constant (with respect to the fix work space coordinate frame xyz, Figure 8).

In the following sections, the kinematics of extender and the mapping of its joints movements based on the two types of constrained motions described above (*i.e.* fixed position, and fixed orientation) are analyzed and discussed.

4.1. Fixed position constraint

This constraint requires the angular velocity vector of grasper ω to vary, while its linear velocity vector $\mathbf{v}$ remain zero. Hence, by using Eq. (2), $\mathbf{v} = \mu + \omega \times \mathbf{a}$, and substituting

https://doi.org/10.1017/S026357479900209X Published online by Cambridge University Press

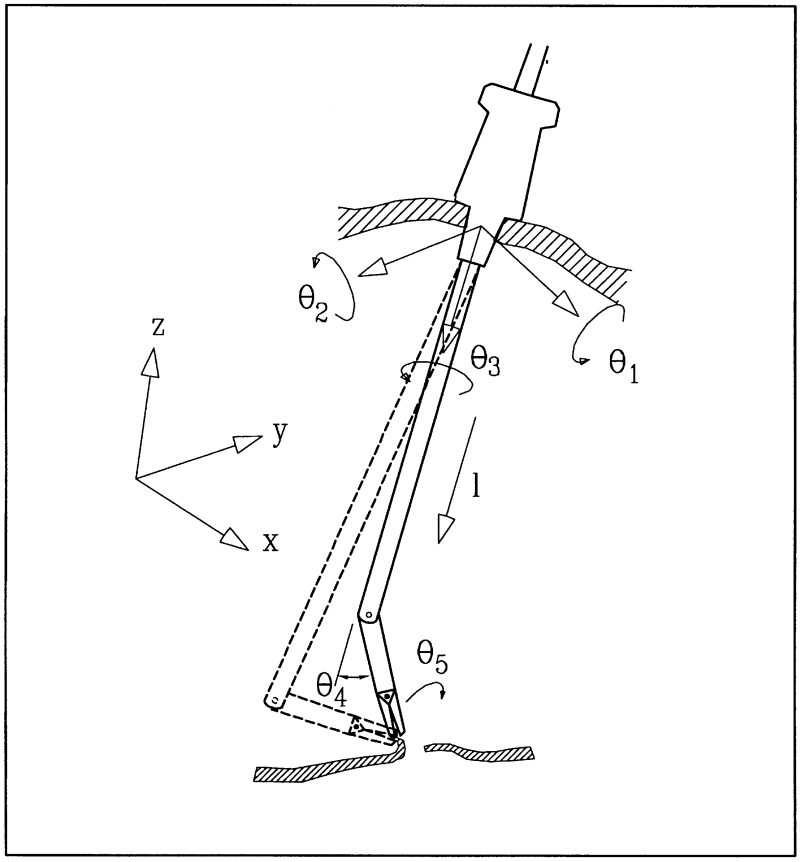

Fig. 7. Fixed position constraint.

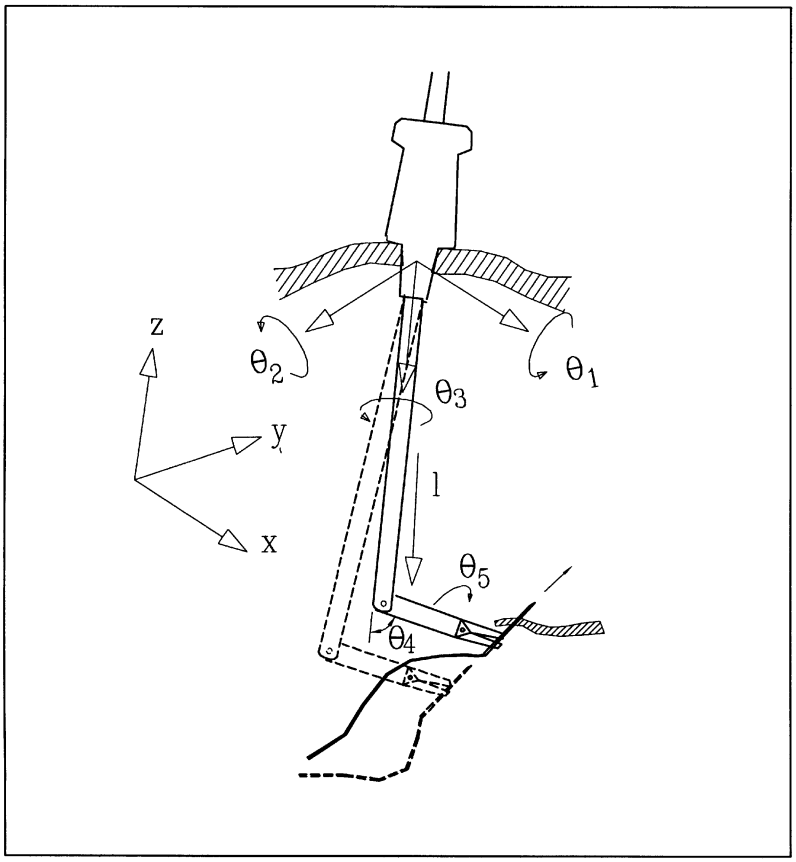

Fig. 8. Fixed orientation constraint.

https://doi.org/10.1017/S026357479900209X Published online by Cambridge University Press

$\mathbf{a} = [l_e S_4 - l_e C_4, 0]^T$ (*i.e.* the position vector of the grasper with respect to the fixed coordinate frame $\mathbf{X}_0$), as well as μ and ω obtained from Eq. (3), we would have:

$$\mathbf{v} = \begin{bmatrix} -lC_2S_3\dot{\theta}_1 + lC_3\dot{\theta}_2 \\ -\dot{l} \\ -lC_2C_3\dot{\theta}_1 - lS_3\dot{\theta}_2 \end{bmatrix} + \begin{bmatrix} C_2C_3\dot{\theta}_1 + S_3\dot{\theta}_2 + S_4\dot{\theta}_5 \\ -S_2\dot{\theta}_1 - \dot{\theta}_3 - C_4\dot{\theta}_5 \\ -C_2S_3\dot{\theta}_1 + C_3\dot{\theta}_2 + \dot{\theta}_4 \end{bmatrix}$$

$$\times \begin{bmatrix} l_e S_4 \\ -l_e C_4 \\ 0 \end{bmatrix} = \begin{bmatrix} 0 \\ 0 \\ 0 \end{bmatrix}$$

This leads us to the following constraint equations:

$$\begin{cases} (l + l_e C_4)(-C_2S_3\dot{\theta}_1 + C_3\dot{\theta}_2) + l_e C_4\dot{\theta}_4 = 0 \\ -\dot{l} + l_e S_4(-C_2S_3\dot{\theta}_1 + C_3\dot{\theta}_2 + \dot{\theta}_4) = 0 \\ (lC_2C_3 + l_eC_2C_3C_4 - l_eS_2S_4)\dot{\theta}_1 + S_3(l + l_eC_4)\dot{\theta}_2 - (l_eS_4)\dot{\theta}_3 = 0 \end{cases}$$

The above equations can be solved for any sets of three variables $\dot{\theta}_1$, $\dot{\theta}_2$, $\dot{\theta}_3$, $\dot{\theta}_4$, or $\dot{l}$, as a function of other remaining variables. However, since the constraints here are related to the fixed position of grasper, we select the positioning axes (*i.e.* θ_1, θ_2, and l) of the extender to be function of orienting axes (*i.e.* θ_3, and θ_4) as follows:

$$\dot{\theta}_1 = \frac{l_e(S_4C_3\dot{\theta}_3 + S_3C_4\dot{\theta}_4)}{C_2(l + l_eC_4) - l_eS_2C_3S_4} \tag{6}$$

$$\dot{\theta}_2 = \frac{-l_eC_4}{C_3(l + l_eC_4)}\dot{\theta}_4 + \frac{C_2S_3}{C_3}\dot{\theta}_1 \tag{7}$$

$$\dot{l} = \frac{l\dot{l}_eS_4}{l + l_eC_4}\dot{\theta}_4 \tag{8}$$

For control purposes of the laparoscopic extender, it is possible to use the above equations when the *fixed position* constraint is desirable for manipulation of tissues. In this case the surgeon can switch the controller to the mode shown by the block diagram Figure 9, so that the positioning axes (*i.e.* θ_1, θ_2 and l) are controlled by orienting axes (*i.e.* θ_3, and θ_4).

The *fix position* constraint is simulated by providing motion for joints θ_3, θ_4, and θ_5, as the orienting axes, and the following constant angular velocities of $\dot{\theta}_3 = \dot{\theta}_5 = 9°/s = 0.157 rad/s$, $\dot{\theta}_4 = 5°/s = 0.0873 rad/s$, from initial coordinates of $[-75°, -75°, -180°, 80mm, -120°, -180°]$ to $[0°, 0°, 0°, 200mm, 20°, 0°]$. By using Eq. 6, 7, and 8, the velocity state of other three slave positioning axes (*i.e.* $\dot{\theta}_1$, $\dot{\theta}_2$, and $\dot{l}$) have been calculated at every 0.1 second time increments. However, it must be pointed out that at each new time increment, the coordinate θ_2 is initially unknown in equations 6, and 7. Therefore, in the first iteration, the coordinate θ_2 of previous time increment is used as a the first approximation, in order to calculate $\dot{\theta}_2$. Then, in the second iteration, θ_2 is calculated by integration of the obtained $\dot{\theta}_2$ over the time increment of 0.1 seconds (Figure 10). After only two iterations, the calculated joint slave velocities $[\dot{\theta}_1, \dot{\theta}_2, \dot{l}]$ converge to such a tolerance that the obtained fix position constraint of end point is satisfied to the level of in the order of a micrometer (*i.e.* $\Delta x = -0.43$, $\Delta_y = -0.12$, *and* $\Delta_z = -1.2$ micrometer) For the full range of the above simulated motion.

For example, in the case of teleoperation master-slave systems, the command values (*i.e.* $\dot{\theta}_3$, $\dot{\theta}_4$ and $\dot{\theta}_5$, Figure 9) can be obtained directly from the measurements of sensors on the master arm's joints which are actuated by the surgeon. On the other hand, the reference coordinates would be used to position control the slave extender while observing the desired kinematic constraint.

4.2. Fixed orientation constraint

In this case, the angular velocity vector of extender ω should remain zero, while the grasper is moving in the work space.

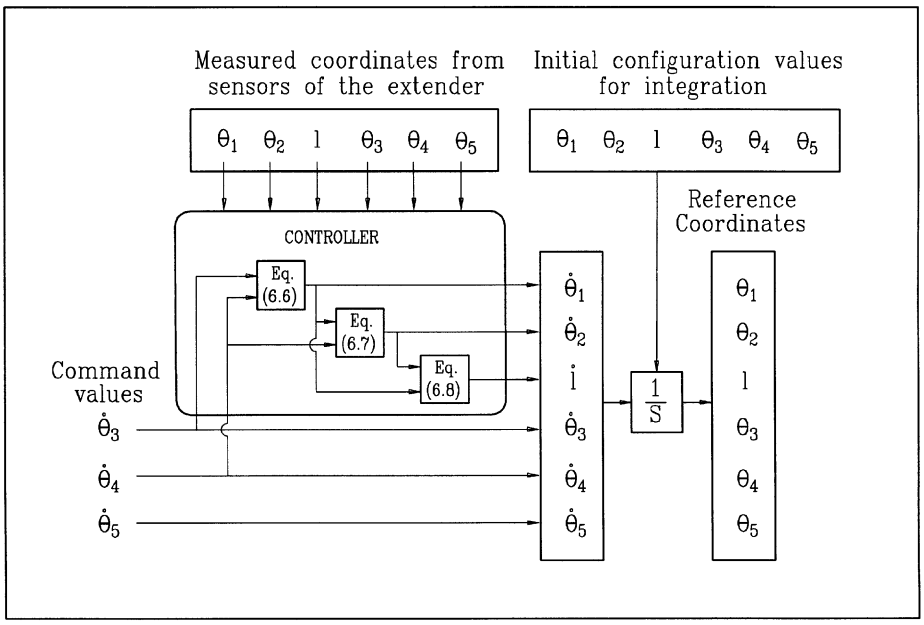

Fig. 9. Block diagram of fixed position controller.

https://doi.org/10.1017/S026357479900209X Published online by Cambridge University Press

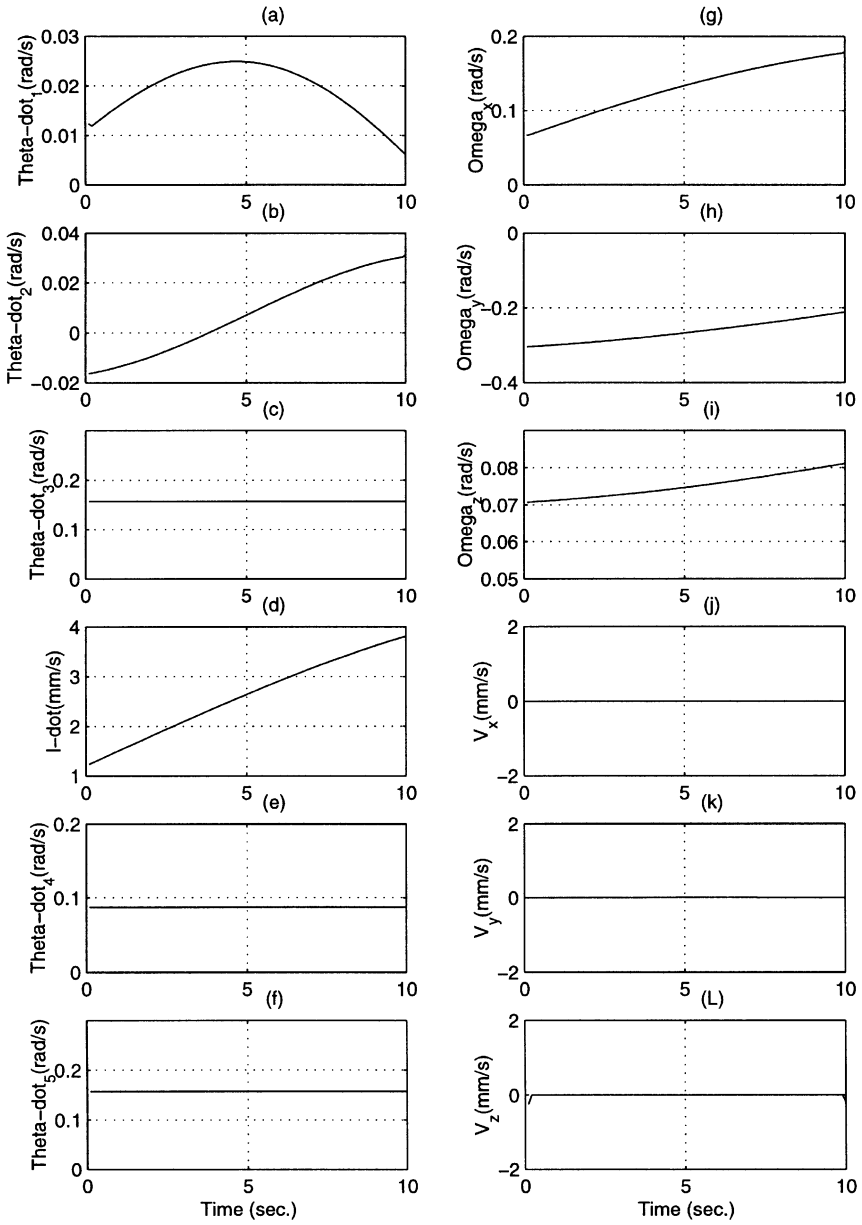

Fig. 10. Simulation of fixed position constrained motion.

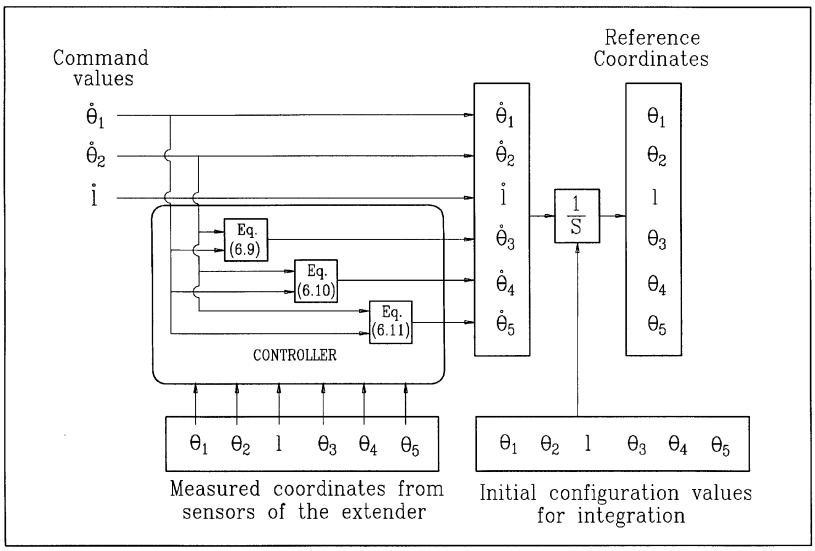

Fig. 11. Block diagram of fixed orientation controller.

https://doi.org/10.1017/S026357479900209X Published online by Cambridge University Press

By using description for ω from Eq. (3) and equating it to zero, we obtain:

$$\begin{cases} \omega_x = 0 = C_2C_3\dot{\theta}_1, + S_3\dot{\theta}_2 + S_4\dot{\theta}_5 \\ \omega_y = 0 = -S_2\dot{\theta}_1 - \dot{\theta}_3 - C_4\dot{\theta}_5 \\ \omega_z = 0 = -C_2S_3\dot{\theta}_1 + C_3\dot{\theta}_2 + \dot{\theta}_4 \end{cases}$$

The above constraints are solved for orienting axes θ_3, θ_4, and θ_5 as a function of positioning axes θ_1, and θ_2 of the extender as follows:

$$\dot{\theta}_3 = -C_4\dot{\theta}_5 - S_2\dot{\theta}_1 = (S_3\dot{\theta}_2 + C_2C_3\dot{\theta}_1)C_4/S_4 - S_2\dot{\theta}_1 \quad (9)$$

$$\dot{\theta}_4 = -C_3\dot{\theta}_2 + C_2S_3\dot{\theta}_1 \quad (10)$$

$$\dot{\theta}_5 = -(S_3\dot{\theta}_2 + C_2C_3\dot{\theta}_1)/S_4 \quad (11)$$

It is possible in this case to use Eqs (9, 10, and 11) to implement the *fixed orientation* constraint by using the control mode shown in the block diagram (Figure 11), so that the orienting axes (*i.e.* θ_3, and θ_4) are controlled by positioning axes (*i.e.* θ_1, and θ_2) as slave axes automatically.

This is simulated similarly by generating constant joints velocities for positioning axes (*i.e.* $\dot{\theta}_1 = \dot{\theta}_2 = 9°/s = 0.157 rad/s$, Figure 12). The initial value of θ_4 for Eq. 9 is obtained from the previous time increment, then after obtaining $\dot{\theta}_4$, it is integrated over time increment of 0.01 sec. to obtain θ_4 for the second iteration. After 4 iterations of $\dot{\theta}_3$, $\dot{\theta}_4$ and $\dot{\theta}_5$, the joints coordinates converge to such a tolerence that the fixed orientation constraint is satisfied to tolerence less than a tenth of degree for the full range of movement (*i.e.* $\Delta\theta_x = 0.071°$, $\Delta\theta_y = 0.001°$, and $\Delta\theta_z = 0.074°$).

In the teleoperation master-slave systems, the command values (*i.e.* $\dot{\theta}_1$, $\dot{\theta}_2$ and $\dot{l}$, Figure 11) can be obtained directly from the measurements of sensors on the master arm's joints which are actuated by the surgeon. On the other hand, the reference coordinates would be used to position control the slave extender while observing the desired kinematic constraint.

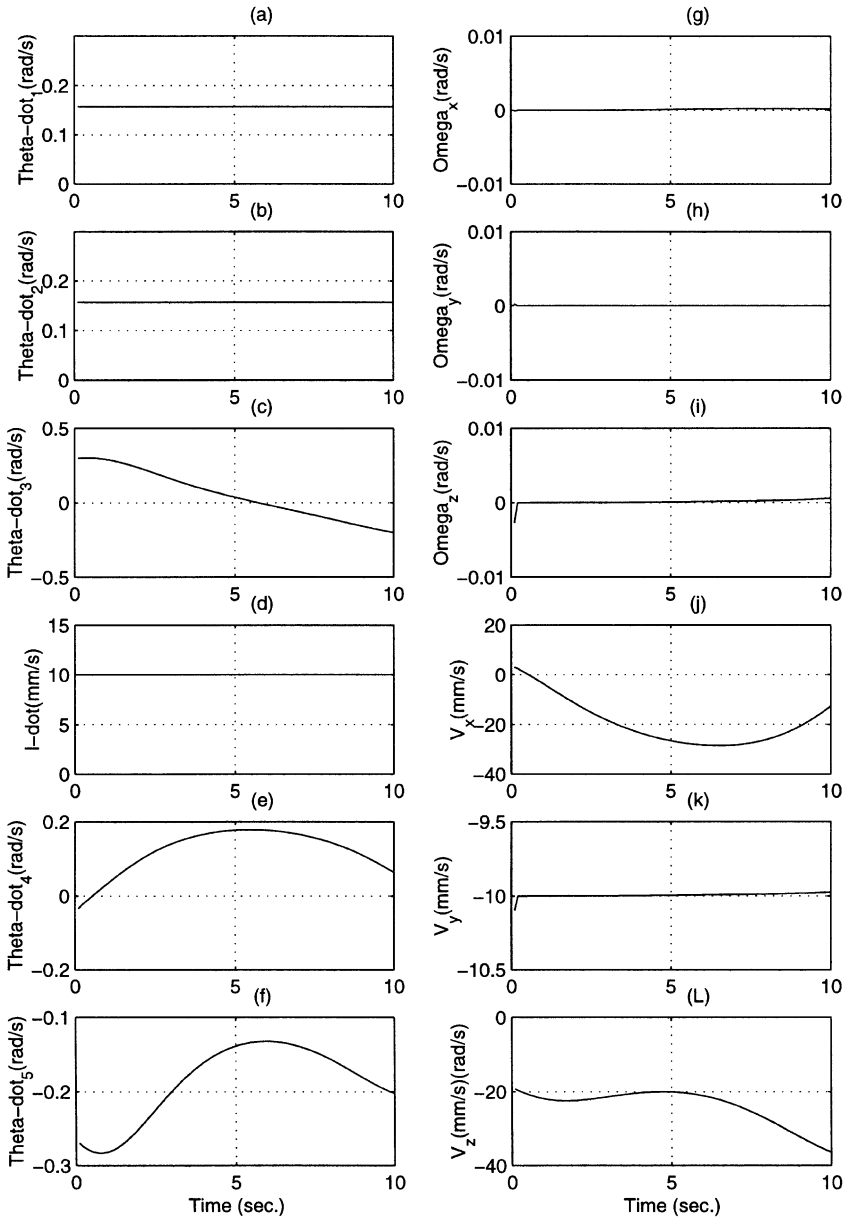

Fig. 12. Simulation of fixed orientation constrained motion.

https://doi.org/10.1017/S026357479900209X Published online by Cambridge University Press

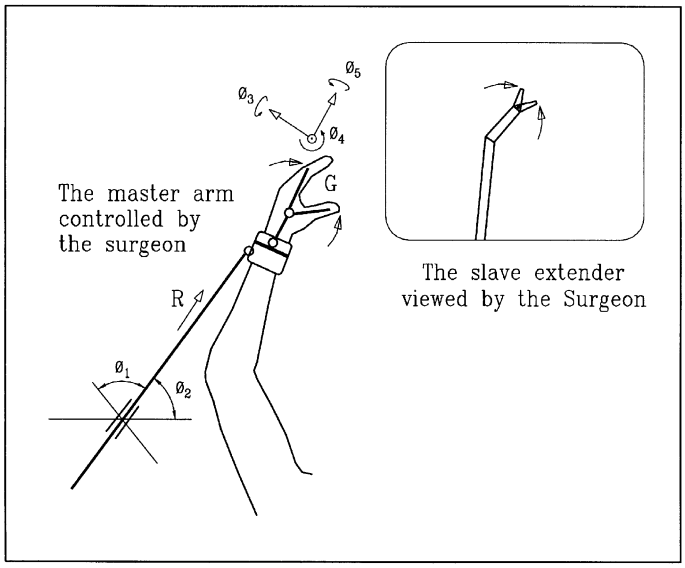

Fig. 13. Schematics of the master arm.

5. CONCLUSION

The main difficulty in laparoscopy is the usage of very long tools through fix small incision points. No matter how much the design of tool (both in terms of degrees of freedom and optimum interface with the surgeon's hand) is improved, still direct physical hand control of the tool is unnatural, remote, and physically demanding. Only with training and practice, it is possible for the surgeon to obtain a fraction of the skill level of open surgery. Therefore to improve dexterity to the level comparable to open surgery, direct hand control of laparoscopic tools cannot be the solution. As a result, further improvement lies in the development of robotic extenders which can be indirectly controlled by the surgeon through a master arm. This master-slave robotic system controls the movements of the robotic extender inside the abdominal cavity, which is controlled indirectly by hand movements of the surgeon on a tele-surgical workstation.[5]

The success of such system not only depends on the general control characteristics of the master-slave system (such as accuracy, fast response, and force reflection) but also its ease of usage by the surgeon. For example to control the extender by means of a "joystick" type of design is not a natural interface for the surgeon, since all the end-effectors movements should be translated to movements of the joystick by logical step by step reasoning, instead of subconscious natural control.

Based on the kinematic study of robotic extenders for laparoscopy, and the above motivation for tele-operation, the following is proposed master/slave configuration subject of future detail design and development. For example, the slave extenders with 6 DOF can be mounted on the arms of a positioning stand.[2] The positioning stand in this case is a passive mechanism that holds the extenders in proper position and orientation with respect to the incision points.

In order to achieve an easy to control master-slave system, which does not require substantial training, it is essential for the slave to mimic hand movements. This means the mechanical movements of the extender should be mapped and controlled by natural movements of human hand. There could be various alternative configurations for the master arm.

The key point in the design configuration of the master arm are:

- The angular orientation of the hand based on the 3 DOF of the wrist to be measured as coordinates ϕ_3, ϕ_4, and ϕ_5 by the master (Figure 13), which are mapped to coordinates θ_3, θ_4, and θ_5 of the slave extender (Figure 2), respectively.
- The positioning coordinate of the hand to be measured (*i.e.* ϕ_1, ϕ_2, and R), and then mapped to the positioning coordinates of the extender (*i.e.* θ_1, θ_2, and l).
- The grasping action of extender to be sensed directly by the angular motion of the thumb G, with respect to other fingers and being reflected directly to the grasper.

References

1. Computer Motion Inc., *AESOP: Automated Endoscopic Systems for Optimal Positioning*, (1994).
2. A. Faraz and S. Payandeh, "A Robotic case Study: Optimal Design of Laparoscopic Positioning Stand," *Int. J. Robotics Research*, **17**, No 9, 986–995 (1998).
3. A. Faraz and S. Payandeh, *Laparoscopic Positioning Stand*, (US Patent ≠5,766,180).
4. R. Taylor, J. Funda *et al*. "A Telerobotic Assistant for laparoscopic Surgery," *IEEE. Engineering in Medicine and Biology Magazine* **14**, 279–288 (1995).
5. A. Faraz and S. Payandeh, "Issues and Design Concepts in Endoscopic Extenders," *Proceedings of 6th IFAC/MMS Symposium*, (1995) pp. 109–114.
6. A. Melzer, "Intelligent Surgical Instrument Systems," *J. Endoscopic Surgery and Allied Technologies* **1**, 165–170 (1993).
7. B. Neisius, P. Dautzenberg and R. Trapp, "Robotic manipulator for Endoscopic handling of Surgical Effectors and Cameras," *Proceedings of 1st International Conference on Medical Robotics and Computer Assisted Surgery*, (1994) pp. 1–7.
8. P. Green, J. Hill and A. Shah, "Telepresence Surgery," *IEEE. Engineering in Medicine and Biology Magazine* **14**, 324–320 (1995).

https://doi.org/10.1017/S026357479900209X Published online by Cambridge University Press

9. K. Waldron, S. Bolin and S. Wang, "A Study of the Jacobian Matrix of Serial Manipulators," *Transaction of ASME*, **107**, 230–238 (1985).
10. A. Faraz and S. Payandeh, "Synthesis and Work-Space Study of Endoscopic Extenders with flexible Stems," *Transaction of ASME, Journal of Mechanical Design* **119**, No 3, pp. 412–414 (1997).

APPENDIX A

The Jacobian of laparoscopic extender with 6 DOF whose coordinates are $[\theta_1,\theta_2,\theta_3,l,\theta_4,\theta_5]^T$ would be a 6×6 matrix. Based on the conventional method of obtaining the Jacobian, the number of terms in each element of the matrix would become very large, which makes it very difficult to use it in forward or inverse kinematics.

However, there is another Jacobian formulation proposed by Waldron[9] which provides much more compact results. In this method, the fixed frame is located at an intermediate joint instead of its normal location at the base of manipulator, and the Jacobian has the following form:

$$\mathbf{J}=\begin{bmatrix}\mathbf{w}_i\\ \rho_i\times\mathbf{w}_i\end{bmatrix} \tag{12}$$

Based on the notation used by the terms $\mathbf{w}_i$ and ρ_i can be obtained recursively based on the following routine:

$$\begin{aligned}\mathbf{R}_i&=\mathbf{Q}_{i-1}\mathbf{U}_i\\ \mathbf{Q}_i&=\mathbf{R}_i\mathbf{V}_i\\ \mathbf{w}_i&=\mathbf{Q}_{i-1}\mathbf{k}\\ \rho_i&=\rho_{i-1}+\mathbf{R}_{i-1}\mathbf{S}_{i-1}\end{aligned} \tag{13}$$

Where $\mathbf{k}=[0,\,0,\,1]^T$, and the initial conditions are: $\mathbf{Q}_0=\mathbf{I}$, $\rho_0=\mathbf{S}_0=0$. The forms for $\mathbf{U}_i$, $\mathbf{V}_i$, *and* $\mathbf{S}_i$ are:

$$\mathbf{U}_i=\begin{bmatrix}C\theta_i & -S\theta_i & 0\\ S\theta_i & C\theta_i & 0\\ 0 & 0 & 1\end{bmatrix},\ \mathbf{V}_i=\begin{bmatrix}1 & 0 & 0\\ 0 & C\alpha_i & -S\alpha_i\\ 0 & S\alpha_i & C\alpha_i\end{bmatrix},\ \mathbf{S}_i=\begin{bmatrix}a_i\\ 0\\ r_i\end{bmatrix}$$

With the reference frame located at Z_4 (Figure 3), also having parameters θ_i, α_i, a_i, *and* r_i as defined in Table I, and working forward in the direction of axis 5, and 6 based above recursive routine would provide the following results:

$$\mathbf{w}_5=\mathbf{k}=\begin{bmatrix}0\\0\\1\end{bmatrix},\ \rho_5=\begin{bmatrix}0\\0\\0\end{bmatrix},\ \rho_5\times\mathbf{w}_5=\begin{bmatrix}0\\0\\0\end{bmatrix}$$

$$\mathbf{w}_6=\mathbf{U}_5\mathbf{V}_5\mathbf{k}=\begin{bmatrix}C_4 & -S_4 & 0\\ S_4 & C_4 & 0\\ 0 & 0 & 1\end{bmatrix}\begin{bmatrix}1 & 0 & 0\\ 0 & 0 & -1\\ 0 & 1 & 0\end{bmatrix}\begin{bmatrix}0\\0\\1\end{bmatrix}=\begin{bmatrix}S_4\\ -C_4\\ 0\end{bmatrix}$$

$$\rho_6=\rho_5+\mathbf{U}_5\mathbf{S}_5=\begin{bmatrix}0\\0\\0\end{bmatrix}$$

$$\rho_6\times\mathbf{w}_6=\begin{bmatrix}0\\0\\0\end{bmatrix}$$

Now, moving inward along the chain toward axis 3, 2, and 1 we obtain:

$$\mathbf{w}_4=\mathbf{V}_4^T\mathbf{U}_4^T\mathbf{k}=\begin{bmatrix}1 & 0 & 0\\ 0 & 0 & -1\\ 0 & 1 & 0\end{bmatrix}\begin{bmatrix}1 & 0 & 0\\ 0 & 1 & 0\\ 0 & 0 & 1\end{bmatrix}\begin{bmatrix}0\\0\\1\end{bmatrix}=\begin{bmatrix}0\\ -1\\ 0\end{bmatrix}$$

$$\rho_4=\rho_5-\mathbf{V}_4^T\mathbf{S}_4=0-\begin{bmatrix}1 & 0 & 0\\ 0 & 0 & -1\\ 0 & 1 & 0\end{bmatrix}\begin{bmatrix}0\\0\\l\end{bmatrix}=\begin{bmatrix}0\\l\\0\end{bmatrix}$$

$$\rho_4\times\mathbf{w}_4=\begin{bmatrix}0\\l\\0\end{bmatrix}\times\begin{bmatrix}0\\ -1\\ 0\end{bmatrix}=\begin{bmatrix}0\\0\\0\end{bmatrix}$$

$$\mathbf{w}_3=\mathbf{V}_4^T\mathbf{U}_4^T\mathbf{V}_3^T\mathbf{U}_3^T\mathbf{k}=\begin{bmatrix}1 & 0 & 0\\ 0 & 0 & -1\\ 0 & 1 & 0\end{bmatrix}\begin{bmatrix}C_3 & S_3 & 0\\ -S_3 & C_3 & 0\\ 0 & 0 & 1\end{bmatrix}\begin{bmatrix}0\\0\\1\end{bmatrix}$$

$$=\begin{bmatrix}0\\ -1\\ 0\end{bmatrix}$$

$$\rho_3=\rho_4-\mathbf{V}_4^T\mathbf{U}_4^T\mathbf{V}_3^T\mathbf{S}_3=\begin{bmatrix}0\\l\\0\end{bmatrix}-\begin{bmatrix}1 & 0 & 0\\ 0 & 0 & -1\\ 0 & 1 & 0\end{bmatrix}\begin{bmatrix}1 & 0 & 0\\ 0 & 1 & 0\\ 0 & 0 & 1\end{bmatrix}\begin{bmatrix}0\\0\\0\end{bmatrix}$$

$$=\begin{bmatrix}0\\l\\0\end{bmatrix}$$

$$\rho_3\times\mathbf{w}_3=\begin{bmatrix}0\\l\\0\end{bmatrix}\times\begin{bmatrix}0\\ -1\\ 0\end{bmatrix}=\begin{bmatrix}0\\0\\0\end{bmatrix}$$

$$\mathbf{w}_2=\mathbf{V}_4^T\mathbf{U}_4^T\mathbf{V}_3^T\mathbf{U}_3^T\mathbf{V}_2^T\mathbf{U}_2^T\mathbf{k}$$

$$=\begin{bmatrix}1 & 0 & 0\\ 0 & 0 & -1\\ 0 & 1 & 0\end{bmatrix}\begin{bmatrix}C_3 & S_3 & 0\\ -S_3 & C_3 & 0\\ 0 & 0 & 1\end{bmatrix}\begin{bmatrix}1 & 0 & 0\\ 0 & 0 & 1\\ 0 & -1 & 0\end{bmatrix}$$

$$\begin{bmatrix}S_2 & -C_2 & 0\\ C_2 & S_2 & 0\\ 0 & 0 & 1\end{bmatrix}\begin{bmatrix}0\\0\\1\end{bmatrix}$$

$$=\begin{bmatrix}S_3\\0\\C_3\end{bmatrix}$$

$$\rho_2=\rho_3-\mathbf{V}_4^T\mathbf{U}_4^T\mathbf{V}_3^T\mathbf{U}_3^T\mathbf{V}_2^T\mathbf{S}_2=\begin{bmatrix}0\\l\\0\end{bmatrix}$$

https://doi.org/10.1017/S026357479900209X Published online by Cambridge University Press

$$\rho_2 \times \mathbf{w}_2 = \begin{bmatrix} 0 \\ l \\ 0 \end{bmatrix} \times \begin{bmatrix} S_3 \\ 0 \\ -C_3 \end{bmatrix} = \begin{bmatrix} lC_3 \\ 0 \\ -lS_3 \end{bmatrix}$$

$$\mathbf{w}_1 = \mathbf{V}_4^T \mathbf{U}_4^T \mathbf{V}_3^T \mathbf{U}_3^T \mathbf{V}_2^T \mathbf{U}_2^T \mathbf{V}_1^T \mathbf{U}_1^T \mathbf{k}$$

$$= \begin{bmatrix} 1 & 0 & 0 \\ 0 & 0 & -1 \\ 0 & 1 & 0 \end{bmatrix} \begin{bmatrix} C_3 & S_3 & 0 \\ -S_3 & C_3 & 0 \\ 0 & 0 & 1 \end{bmatrix} \begin{bmatrix} 1 & 0 & 0 \\ 0 & 0 & 1 \\ 0 & -1 & 0 \end{bmatrix}$$

$$\begin{bmatrix} S_2 & -C_2 & 0 \\ C_2 & S_2 & 0 \\ 0 & 0 & 1 \end{bmatrix} \begin{bmatrix} 1 & 0 & 0 \\ 0 & 0 & -1 \\ 0 & 1 & 0 \end{bmatrix} \begin{bmatrix} C_1 & S_1 & 0 \\ -S_1 & C_1 & 0 \\ 0 & 0 & 1 \end{bmatrix} \begin{bmatrix} 0 \\ 0 \\ 1 \end{bmatrix}$$

$$= \begin{bmatrix} C_2 C_3 \\ -S_2 \\ -C_2 S_3 \end{bmatrix}$$

$$\rho_1 = \rho_2 - \mathbf{V}_4^T \mathbf{U}_4^T \mathbf{V}_3^T \mathbf{U}_3^T \mathbf{V}_2^T \mathbf{U}_2^T \mathbf{V}_1^T \mathbf{S}_2 = \begin{bmatrix} 0 \\ \ell \\ 0 \end{bmatrix}$$

$$\rho_1 \times \mathbf{w}_1 = \begin{bmatrix} 0 \\ \ell \\ 0 \end{bmatrix} \times \begin{bmatrix} C_2 C_3 \\ -S_2 \\ -C_2 S_3 \end{bmatrix} = \begin{bmatrix} -\ell C_2 S_3 \\ 0 \\ -\ell C_2 C_3 \end{bmatrix}$$

Therefore the final Jacobian after assembling all $\mathbf{w}_i$ and $\rho_i \times \mathbf{w}_i$ elements in the form of 6×6 matrix would be:

$$\mathbf{J} = \begin{bmatrix} \mathbf{w}_i \\ \rho_i \times \mathbf{w}_i \end{bmatrix} = \begin{bmatrix} C_2 C_3 & S_3 & 0 & 0 & 0 & S_4 \\ -S_2 & 0 & -1 & 0 & 0 & -C_4 \\ -C_2 S_3 & C_3 & 0 & 0 & 1 & 0 \\ -lC_2 S_3 & IC_3 & 0 & 0 & 0 & 0 \\ 0 & 0 & 0 & -1 & 0 & 0 \\ -lC_2 C_3 & -lS_3 & 0 & 0 & 0 & 0 \end{bmatrix} \tag{14}$$

https://doi.org/10.1017/S026357479900209X Published online by Cambridge University Press